Influence of ion migration from ITO and SiO_2 substrates on photo and thermal stability of $CH_3NH_3SnI_3$ hybrid perovskite

Ivan S. Zhidkov[1]*, *Danil W. Boukhvalov*[2,1], *Andrey I. Kukharenko*[1], *Larisa D. Finkelstein*[3], *Seif O. Cholakh*[1], *Azat F. Akbulatov*[4], *Emilio Jose Juarez-Perez*[5], *Pavel A. Troshin*[6,4], *and Ernst Z. Kurmaev*[1,3]

1 – Institute of Physics and Technology, Ural Federal University, Mira Str. 19, 620002, Yekaterinburg, Russia

2 – College of Science, Institute of Materials Physics and Chemistry, Nanjing Forestry University, 210037 Nanjing, P. R. China

3 – M.N.Mikheev Institute of Metal Physics of Ural Branch of Russian Academy of Sciences, S.Kovalevskoi Str. 18., 620108 Yekaterinburg, Russia

4 – Institute for Problems of Chemical Physics of the Russian Academy of Sciences (IPCP RAS), Semenov Ave. 1, 142432 Chernogolovka, Russia

5 – ARAID, Government of Aragon, Institute of Nanoscience of Aragon (INA), University of Zaragoza, 50018 Zaragoza, Spain.

6 – Skolkovo Institute of Science and Technology, Nobel Str. 3, 143026 Moscow, Russia

KEYWORDS: hybrid perovskites, XPS, light-induced degradation, photostability, thermal stability.

Abstract. The effect of ion migration from indium tin oxide (ITO) and SiO_2 substrates on the photo and thermal degradation of $CH_3NH_3SnI_3$ hybrid perovskite is studied. The measurements of X-ray photoelectron survey spectra (XPS) showed an increase in the concentration of substrate ions in the surface layer of ITO/$CH_3NH_3SnI_3$ and reduction of N:Sn and I:Sn ratios after 500 hours of white light irradiation and 200 hours of annealing at 90 ºC. The high-energy resolved XPS Sn 3d-spectra of ITO/$CH_3NH_3SnI_3$ indicated a consistent increase in the contribution of Sn^{4+}-ions at these exposure times under light-soaking and heat stress. The nature of this phenomenon was established on the basis of XPS Sn 3d, O 1s and valence band (VB) measurements and density functional theory (DFT) calculations that revealed that at the initial stages of $CH_3NH_3SnI_3$ degradation, the SnI_4 phase separation occurs and with a further increase in exposure time, tin is oxidized to form a SnO_2 phase. In order to check the effect of SiO_2 substrate on the SiO_2/$CH_3NH_3SnI_3$ resistance to external influences, we chosed annealing at 300 hours since the thermal degradation is clearly visible already at 200 hours for ITO/$CH_3NH_3SnI_3$ sample. The Sn 3d, O 1s and VB spectra from XPS showed that for $CH_3NH_3SnI_3$ perovskite the SiO_2 substrate is more stable than ITO and the effect of the oxidation of tin atoms due to the migration of oxygen ions is very weak. The theoretical modeling demonstrates that formation of SnI_2 defects in $CH_3NH_3SnI_3$ became irreversible due to the oxidation by migration of the oxygen

ions from substrate. The calculated formation energy of oxygen vacancy in ITO is about two times smaller than in SiO_2 that explains an instability of ITO/$CH_3NH_3SnI_3$.

1. Introduction

Hybrid lead halide perovskites have attracted a great attention last years because of their pronounced progress in optoelectronic applications.[1-2] After 9 years of development the power conversion efficiency (PCE) of perovskite solar cells (PSC) based on these materials increased from 3.9 to 25.2% which is comparable with that of traditional silicon-based solar cells.[3] However, the toxicity problem of lead halide perovskites limits their practical large-scale commercialization.[4] One of the way to solve this problem is to replace Pb with the less toxic Sn or Ge to form the perovskites[5] and few years ago Stoumpos et al.[6] reported $CH_3NH_3SnI_3$-based perovskite solar cells with a PCE of $\approx 6\%$. Although the optical and electronic properties of Sn-based perovskites are highly attractive, the instability of these materials to moisture, light and heat restricts their practical applications. Sn^{2+} ions in $CH_3NH_3SnI_3$ perovskites are easily oxidized to Sn^{4+} and even less than 0.1% Sn^{4+} doping induces the degradation of the solar cell performance.[7-8] It has been found that the addition of SnF_2 prevented the degradation of tin-based perovskites.[9] However, such prevention is rather limited and in connection with this, the understanding the origin of degradation of complex tin halides and developing stable Sn-based perovskite electronic devices with good reproducibility is very important.[10] An essential result of the problem under consideration is the dependence of the bulk properties of hybrid perovskite films on the type of substrate used for film growth. It was established that the roughness and nature of the substrate and deposited layer (glass, ITO, TiO_2, and PEDOT: PSS) affects not only

the degree of preferred orientation and crystalline grain size but also varying lattice parameters and specially distance between Pb-Pb metal atoms to ±0.7%. It is also assumed that the chemical nature of the substrate and selective layer thin-film affects the concentration of defects and the inclusion of oxygen and iodine vacancies during the nucleation and growth of the perovskite film. These variables must have direct consequences in the observed degradation caused by light and heat in perovskite. It has been shown that laser illumination leads to the formation of additional defects, primarily those associated with oxygen which is recorded by measurements of the Raman spectra.[11] It is also discussed the possibility of changing the chemical composition in the perovskite layer due to the migration of ions from the substrate under the influence of light and temperature which can affect the chemical reactions that occur in the perovskite layer.[12] In relation to tin-based hybrid perovskites, the particular interest is the migration of oxygen ions from the ITO and SiO_2 substrates and the degradation of the hybrid perovskite layer caused by this process. In connection with this, we are studying in the present paper the influence of oxygen ion migration from substrate into ITO/$CH_3NH_3SnI_3$ and SiO_2/$CH_3NH_3SnI_3$ samples induced by light soaking and heat stress and tracking changes using XPS spectra (survey, core level and valence band spectra). To exclude the effect of oxidation in air, all samples for photoemission studies were sealed in special containers (sliders), which were opened just before they were installed in the spectrometer, in order to minimize their time in the air before performing spectral experiments. In such a way, XPS spectra of ITO/$CH_3NH_3SnI_3$, SiO_2/$CH_3NH_3SnI_3$ and reference compounds (SnI_2, SnI_4 and SnO_2) were investigated.

2. Experimental and Calculation Details

ITO and SiO_2 substrates (25×25 mm^2) were sequentially cleaned with toluene and acetone and then sonicated in deionized water, acetone, and isopropanol. The $CH_3NH_3SnI_3$ solutions with a concentration of 0.75 M were prepared by dissolving the corresponding precursors in a mixture of dimethylformamide (DMF) and dimethyl sulfoxide (DMSO) (4:1 v/v). Prepared solutions were spin-coated at 5000 rpm inside a nitrogen glove box. Toluene (100 μL) was added at the 30th second after the start of the spinning, thus quenching the precursor and inducing the film crystallization. Spinning was continued for 30 s more, and then the deposited films were annealed at nitrogen inside the glove box with O_2 < 0.1 ppm and H_2O < 0.1 ppm at 70 °C for 5 min.

Thermal stress tests of the films were performed inside a nitrogen glove box. The samples were placed on the hot plate at 90 °C and covered with a nontransparent lid to avoid their exposure to the ambient light. The light-soaking experiments were performed using a specially designed setup integrated with the dedicated MBraun glove box. We applied a metal-halide lamp as a standard light source, which is known to provide a good approximation of the solar AM1.5G spectrum. Considering the possible UV light effect on the stability of the perovskite films, we applied an additional UV filter to cut-off the wavelengths below 300 nm. The light power at the samples was ∼100 ± 5 mW/cm^2, while the temperature was 65 ± 3 °C (provided by intense fan cooling of the sample stage).

XPS was used to measure survey spectra at binding energies range of 0-650 eV and high-energy resolved O 1s and valence band (VB) spectra with help of a PHI XPS 5000 VersaProbe spectrometer (ULVAC-Physical Electronics, USA) with a spherical quartz monochromator and an energy analyzer working in the range of binding energies from 0 to 1500 eV. The energy

resolution was ✎E ≤ 0.5 eV. The samples were kept in the vacuum chamber for 40 min prior to the experiments and were measured at a pressure of 10^{-7} Pa.

First-principles modelling calculations were performed using the SIESTA computational package.[13] The Perdew-Burke-Ernzerhof variant of the generalized gradient approximation (GGA-PBE)[14] with spin polarization was employed. Relatively large basis set for norm-conserving TM-pseudopotentials[15] are used: for Sn the $5s^2$ $5p^2$ $5d^0$ $5f^0$, for In $5s^2$ $5p^1$ $4d^{10}$ $5f^0$, for I the $5s^2$ $5p^5$ $5d^0$ $4f^0$, for Si the $3s^2$ $3p^2$ $3d^0$, for C the $2s^2$ $2p^2$ $3d^0$, for N the $2s^2$ $2p^3$ $3d^0$, and for O the $2s^2$ $2p^4$ $3d^0$ orbitals are included in the valence. For the indium, corrections of semicore states were taken into account[16]. The forces and total energies were optimized with an accuracy of 0.04 eV $Å^{-1}$ and 1.0 meV, respectively.

The calculations of $CH_3NH_3SnI_3$ were performed on a 3×3×3 supercell (324 atoms, see Figure 1a) similar to use in our previous work on similar systems.[17] The initial lattice parameters were obtained from lattice optimization at zero temperature. Our recent MD modelling demonstrate insignificant expansion of the lattice annealing thus we omit contribution from thermal expansion.[17] To imitate the initial disorder in the thin films hybrid perovskites at finite temperatures, we used quasi-random distribution for the initial orientation of the MA groups. For the modelling of ITO we used the unit cell of In_2O_3 (80 atoms)[18] with random distribution of 2, 4, and 8 substitutional Sn impurities corresponding to 12.5, 25 and 50% of tin amount. For the modeling oxygen vacancies, we compare the energetics of two cell one with vacancy in vicinity of Sn-impurity and another with two distant defects. For the modeling of the oxygen vacancies in SiO_2 we used 2×2×2 supercell of 72 atoms. Energies of the chemical processes were discussed as the differences between total energies of products and reactants. Our recent work demonstrated feasibility of this model for description of defects in quartz.[19] For SnO_2, SnI_2, SnI_4 we calculate

electronic structure and total energies for the structures corresponding with ground states. Molecular oxygen and $CH_3NH_3^+$ were modeled as single molecules in empty boxes.

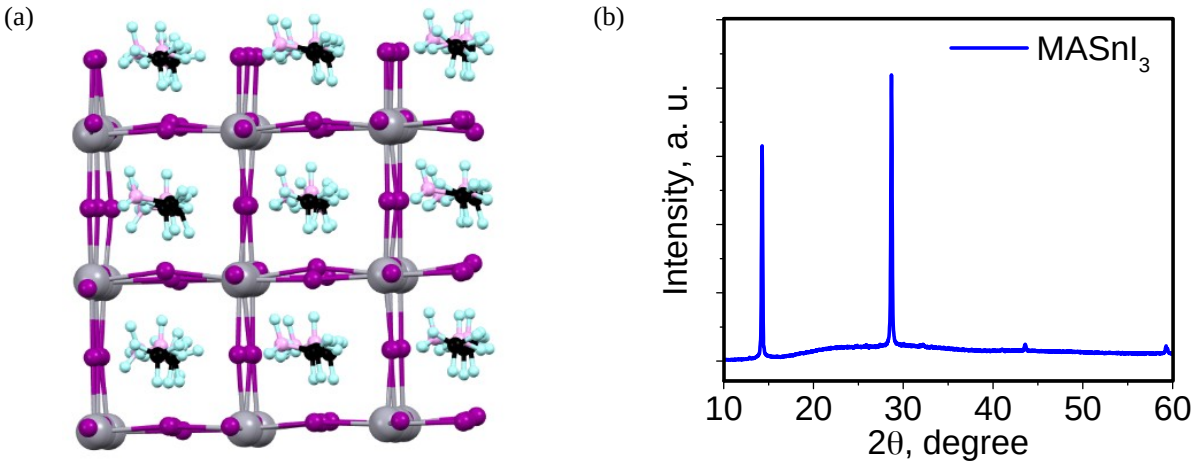

Figure 1. Optimized atomic structure of $CH_3NH_3SnI_3$ supercell. Tin atoms are shown by grey, iodine by violet, carbon by black, nitrogen by light pink and hydrogen by light blue (a). The XRD pattern of deposited $MASnI_3$ film (b).

3. Results and Discussion

3.1 ITO/$CH_3NH_3SnI_3$

X-ray diffraction patterns of $MASnI_3$ shows two peaks at 14.2° and 28.7° typical for (100) and (200) crystallographic planes of cubic perovskite lattice (Figure 1b). Absence of other peaks indicated that the films are highly textured. To study the detailed mechanism of photo-/thermal-degradation of ITO/$CH_3NH_3SnI_3$, we first measured the XPS survey spectra in the energy range of 0-650 eV of irradiated and annealed samples with aging time of 0-1000 hours. The results are presented in Figure 2 and the surface compositions determined from these spectra (a quantitative estimate of the relative concentration of elemental species is obtained from the measured integral

intensities, corrected by the elemental and orbital specific photoemission cross sections are summarized in Table 1 (in at.%).

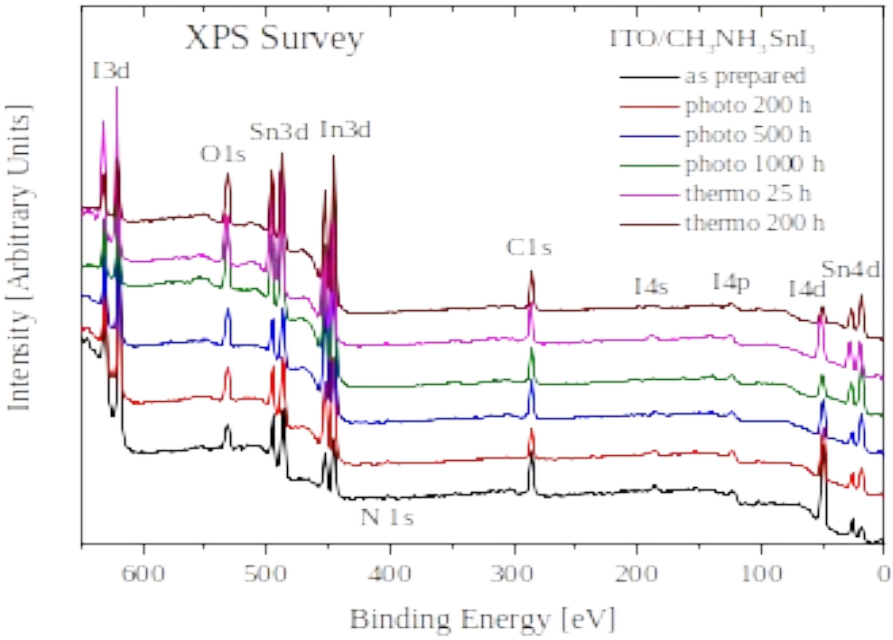

Figure 2. XPS survey spectra of light-soaking and heat stressed ITO/$CH_3NH_3SnI_3$ hybrid perovskites.

Table 1. Surface composition of the as-prepared, light irradiated, and annealed ITO/$CH_3NH_3SnI_3$ samples (in at.%).

ITO/$MASnI_3$	**C**	**O**	**I**	**Sn**	**N**	**In**	**F**	**Si**	**N:Sn**	**I:Sn**	**O:Sn**
As prepared	56,3	15,6	12	4,5	4,9	3,8	-	2,9	1,08	2,66	3,47
Photo-200 h	41,2	24,6	12,5	6	3,7	9,5	-	2,5	0,61	2,08	4.10
Photo-500 h	45,6	24,8	8,6	4,9	2,3	12,6	-	1,2	0,46	1,75	5,06
Photo-1000 h	34,3	37,6	4,8	7,8	1,2	13,9	-	-	0,15	0,61	4,82

Thermo-25 h	43,8	27,1	8,3	8,7	1,6	9,3	1,2	-	0,18	0,95	3,12
Thermo-200 h	42,1	32,3	3,4	7,4	-	12,8	2	-	-	0.45	4,36

Overall, the elements belonging to the perovskite (C, N, Sn and I) and the substrate (In and O) were found on the surface of the studied samples. This means that the prepared perovskite layers do not fully cover the ITO-substrate and have some voids (or pin-holes) through which the substrate elements are visible in XPS substrate spectra even in as prepared sample. To approve this suggestion, we also applied the scanning electron microscopy (SEM) to observe the morphology of the surface (Figure 3). As seen from these data, an increase in the concentration of substrate ions (In, Sn and O) in the ITO/$CH_3NH_3SnI_3$ surface layer after 200 h aging time may be due to two factors - an increase in the size of voids due to decomposition of the organic cation and the diffusion of substrate elements onto the surface of the perovskite layer. The reduction of N:Sn and I:Sn ratios indeed means the loss of organic cation ($CH_3NH_3^+$) and change of I-Sn bonds. Instead, C 1s is not valid signal to track the organic cation because it is affected of adventitious carbon. Overall, XPS results are consistent with the $CH_3NH_3SnI_3$ perovskite degradation mechanism proposed in the literature.[20-21] As shown in the XRD measurements of both photo- and thermal-aged perovskite films,[10] the decomposition of $CH_3NH_3SnI_3$ is evidenced by the disappearance of associated diffraction peaks accompanied with the appearance of SnI_2 peak.

As follows from this mechanism, one of the products of degradation is SnI_4 compound which contains the tetravalent Sn-ions. The transition from bivalent in the initial perovskite ($CH_3NH_3Sn^{2+}I_3$) to tetravalent in $Sn^{4+}I_4^-$ product of decomposition should be recorded in the XPS

Sn 3d-spectra. To verify this, we measured high-energy resolved XPS Sn 3d-spectra in as prepared, light-soaked (Figure 4a), and annealed (Figure 4b) $CH_3NH_3SnI_3$ films.

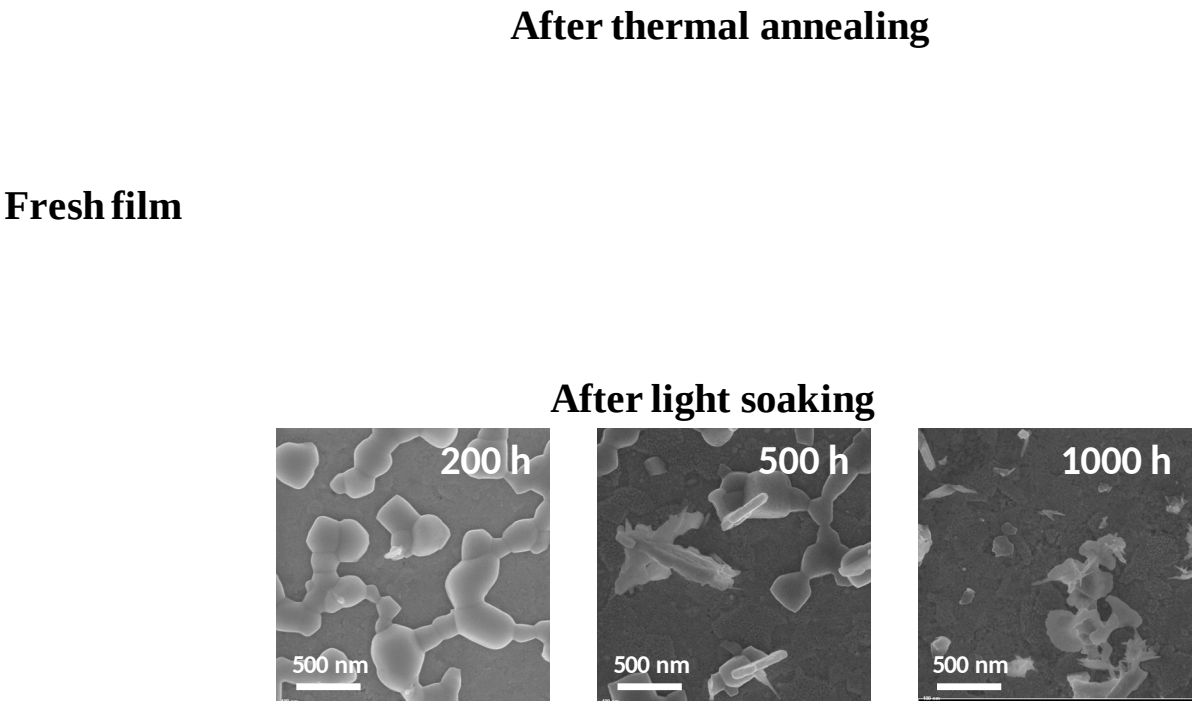

Figure 3. Changing of morphology of $MASnI_3$ films after thermal and photochemical aging.

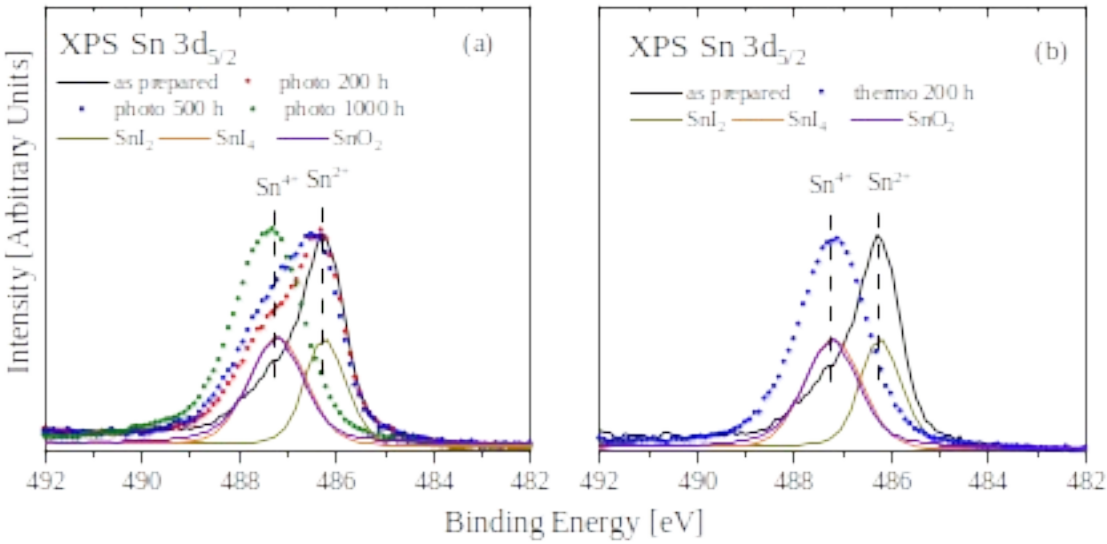

Figure 4. XPS Sn $3d_{5/2}$-spectra of light soaking (a) and heat stressed (b) ITO/$CH_3NH_3SnI_3$.

Indeed, as can be seen from these data, the binding energy of the XPS Sn $3d_{5/2}$-spectrum in the initial perovskite coincides with that in the reference SnI_2 compound with divalent tin ions, while irradiation with visible light and annealing lead to the appearance of a high-energy feature which ultimately forms into an independent peak coinciding at large exposure times in energy with that of the SnI_4 and SnO_2 compounds.

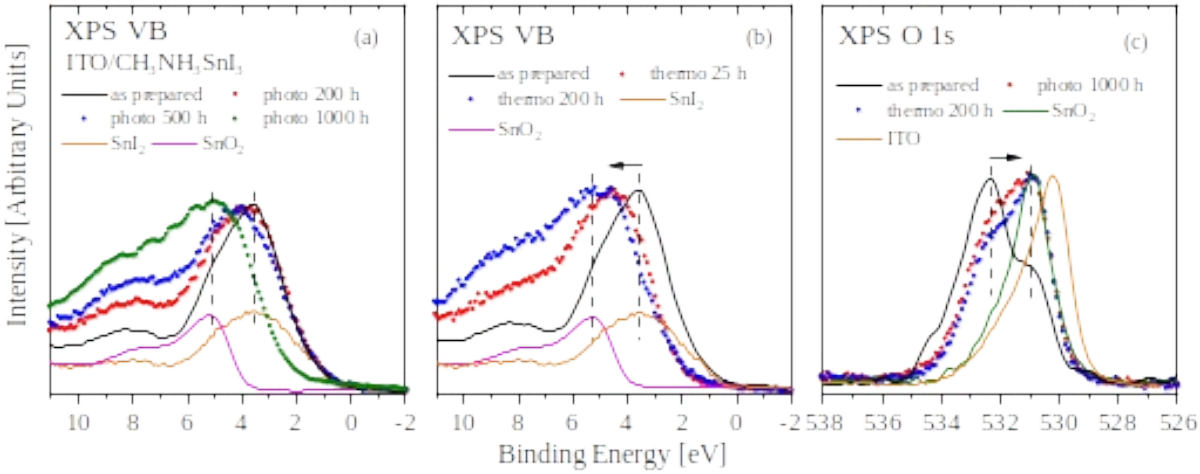

Figure 5. XPS VB spectra of light irradiated (a) and annealed (b) ITO/$CH_3NH_3SnI_3$ samples and XPS O 1s (c) of ITO/CH3NH3SnI3 before and after photo and thermal treatment.

We further examined how the light-soaking and heat stress affect the XPS valence band spectra. As follows from Figures 5a-b, an increase in the time of these external influences leads to a high-energy shift of the maximum intensity of the XPS valence band spectra. It is important noting that threshold values of degradation expressed in terms of energy shift of XPS VB exactly

coincide with those determined from the I:Sn ratios and XPS Sn 3d-spectra (see Table 1 and Figure 4) and correspond to 500 hours and 200 hours for irradiation with visible light and annealing, respectively. For high exposure times, this shift leads to the actual coincidence of the XPS Sn 3d-spectrum with that in the SnO_2 compound for light soaking at 1000 h and heat stress at 200 h. In connection with this let us return again to the Table 1. A progressive increase in the indium and oxygen concentrations with aging time is noticeable both upon irradiation with visible light and under annealing. For example, with an increase in the light irradiation time from 0 to 1000 hours, the indium, tin and oxygen content in the surface layer increased from 3.8, 4.5 and 15.6 to 13.9, 7.8 and 37.6 at.%, respectively. A similar effect is observed during annealing where an increase in exposure time to 200 hours leads to an increase in similar concentrations to 12.8, 7.4 and 32.3 at.%, respectively (see Table 1). As we noted above, this can be caused by both the degradation of the organic cation and, as a result, a change in morphology due to an increase in the size of voids and by diffusion of the substrate elements on the surface of the perovskite layer induced by light irradiation and annealing. This process in Table 1 corresponds to a decrease in N:Sn, I:Sn and an increase in O:Sn. . It should be noted that migration of indium ions from the ITO substrate to the surface of the deposited perovskite layer it was also previously reported in literature. [22-23] The theoretical approach proposed in Section 3.3 to the mechanism of perovskite degradation is based on the formation of SnI_2 vacancies as a result of oxidation of SnI_2 by oxygen from the substrate based on the measurement of the O:Sn ratio. A convincing illustration of the migration of oxygen ions from the substrate to the surface of the perovskite layer and their interaction with metal atoms is given in Figure 5c, which shows the oxygen spectra of the initial sample and after irradiation with visible light and annealing. If photo irradiation and annealing only lead to an increase of the voids in the perovskite layer, then one

could expect the appearance of the oxygen spectrum of the corresponding ITO-substrate. However, as can be seen from this figure, the measured oxygen spectra differ significantly from that of ITO-substrate and coincides with the spectrum of the oxygen in the SnO_2-oxide. It follows from XPS O1s-spectra (Fig. 5c) that the surface of the initial sample irradiated with visible light and annealed is coated with adsorbed oxygen (532.3 eV) near which the peak of SnO_2 (530.9 eV) grows with aging time. Oxygen adsorption probably occurs at the moment the sample is introduced into the working chamber of the spectrometer.

Thus, the mechanism of ITO/$CH_3NH_3SnI_3$ perovskite degradation can be represented in two stages. At the first stage, at low aging times, the photochemical and thermochemical decomposition of the $CH_3NH_3SnI_3$ compound probably occurs with the formation of the SnI_4 compound as a decomposition product. With an increase in the exposure time, oxygen atoms diffuse from the ITO-substrate and the process is complicated by the additional formation of tetravalent tin ions due to the oxidation of tin atoms (see Refs 20-21, 24).

3.2 $SiO_2/CH_3NH_3SnI_3$

The surface composition of annealed $SiO_2/CH_3NH_3SnI_3$ (Table 2) determined from XPS survey spectrum (Figure 6) showed that the N:Sn and I:Sn ratios are much higher (0.34 and 1.86) than those in the annealed at 200 h ITO/$CH_3NH_3SnI_3$ sample (0 and 0.45) whereas O:Sn ratio in opposite is decreased (3.22 and 4.36) (see Table 1). This definitely indicates that almost at certain exposure times (20-300 hours) there is a higher thermal stability of the $CH_3NH_3SnI_3$ prepared on the SiO_2 substrate.

Table 2. Surface composition of annealed $SiO_2/CH_3NH_3SnI_3$ sample (in at.%).

$SiO_2/MASnI_3$	C	O	I	Sn	N	F	Na	Si	N:Sn	I:Sn	O:Sn
Thermo-300 h	41,20	23,50	13,60	7,30	2,50	0,80	4,0	7,10	0,34	1,86	3,22

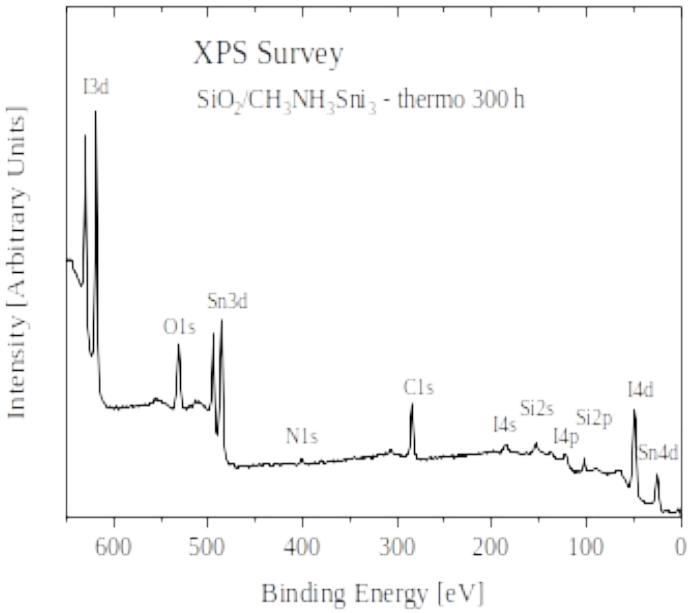

Figure 6. XPS survey spectra of heat stressed $SiO_2/CH_3NH_3SnI_3$ hybrid perovskite.

This conclusion is also confirmed by comparing the XPS Sn $3d_{5/2}$, O 1s and VB-spectra measured for the $SiO_2/CH_3NH_3SnI_3$ and $ITO/CH_3NH_3SnI_3$ samples (see Figures. 7a-c).

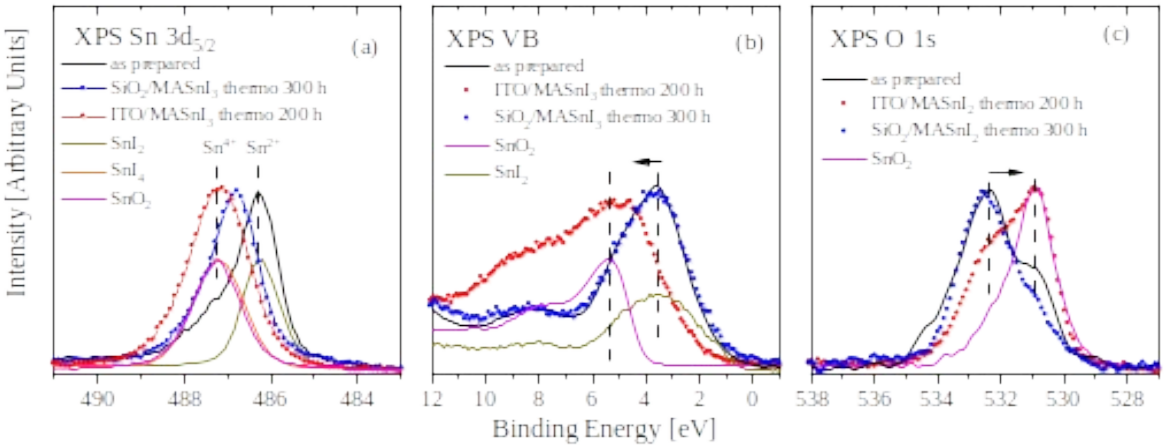

Figure 7. Comparison of XPS Sn $3d_{5/2}$ (a), VB (b) and O 1s (c) spectra of pristine and heat stressed ITO/$CH_3NH_3SnI_3$ and SiO_2/$CH_3NH_3SnI_3$.

As follows from Figure 7a, if a high-energy shift of XPS Sn $3d_{5/2}$ of 0.84 eV of towards the reference SnI_4 compound (1.0 eV) is observed during annealing of the ITO/$CH_3NH_3SnI_3$ sample, then for the SiO_2/$CH_3NH_3SnI_3$ this shift is only 0.52 eV.

The comparison of the XPS VB spectra of ITO/$CH_3NH_3SnI_3$ and SiO_2/$CH_3NH_3SnI_3$ compounds shows that with equal heat treatment the spectrum of ITO/$CH_3NH_3SnI_3$ is shifted toward the high energy side and coincides in position with that in the $Sn^{4+}O_2$ since the XPS VB of SiO_2/$CH_3NH_3SnI_3$ does not show such a shift and coincides in position with the spectrum of the reference $Sn^{2+}I_2$ (see Figure 7b). The final point in the comparison of the spectra of these two compounds was put in Fig. 6c where the XPS O 1s-spectra are presented. These results show that unlike the ITO/$CH_3NH_3SnI_3$ where the annealing leads to the appearance of a high-intensity component close in energy to the SnO_2 oxide spectrum in the SiO_2/$CH_3NH_3SnI_3$ compound, no such modification of the XPS O 1s-spectrum is observed.

3.3 DFT modelling

At the first step of our modeling we checked the formation energies corresponding to formation of SnI_2 phase. We described the formation of SnI_2 phase as the process started from the formation of SnI_2 vacancies in the supercell shown in Figure 1. We also checked relationships between energetics and concentration of the vacancies. For the defect concentration of 3.7 at%, the formation energy is -0.37 eV/SnI_2. The further increasing of the defect concentration up to 7.4 at% and 11.1 at% provides the increase of the formation energies to -0.04 and +0.15 eV/SnI_2, correspondingly. This process can be considered as reversible. Irreversibility of this process can be related with oxidation of SnI_2 by the oxygen from the air or substrate. Before discussion of this process we checked the influence of the formation of SnI_2 defects on electronic structure. At the concentration 11.1 at% of SnI_2 vacancies the shift of the main peak of valence band at about 0.25 eV from Fermi level is observed (Figure 8). This change in electronic structure corresponds to experimentally observed slight shift of this peak at initial stages of photo-degradation (200 and 500 hours, see Figure 5a) and 25 hours of thermo-degradation of ITO/$CH_3NH_3SnI_3$ (Figure 5b).

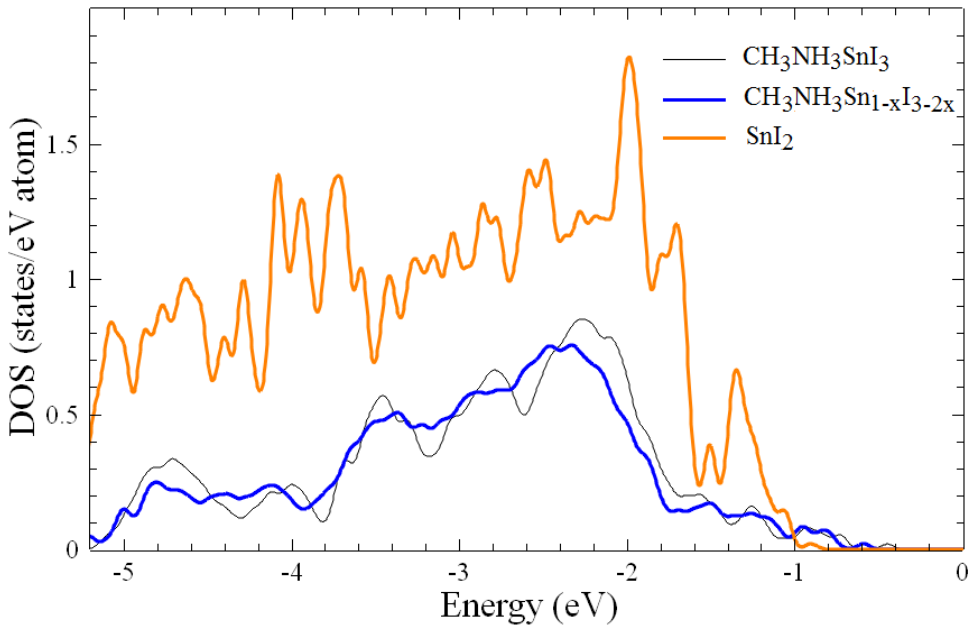

Figure 8. Calculated densities of states for undefected $CH_3NH_3SnI_3$, the same supercell with three SnI_2 vacancies (11.1 at%) and bulk SnI_2.

In the absence of oxygen from the air, its source may be an oxygen-containing substrate. For evaluation of the favorability of the proposed degradation pathway we have calculated the energy of the formation the oxygen vacancies in both materials used as substrates (ITO and SiO_2). The formation energy of the single oxygen vacancy in SiO_2 is found to be rather high (+5.18 eV/O). The energy cost of creating of the oxygen vacancy in ITO depends from the tin concentration. The calculated values are +4.79, +4.09 and +2.77 eV/O for 12.5, 25 and 50% concentration of tin. Thus in the case of ITO-substrate the producing of the oxygen for reaction can be always energetically cheaper than for glass substrate. Note that according to Arrhenius equation the yield of reaction depends from the energy cost exponentially, therefore the decomposition $CH_3NH_3SnI_3$ on ITO substrate will be about from 1.5 to 11 times faster than over glass substrate.

4. Conclusions

In conclusion, it was demonstrated that, when exposed to visible light and annealing, the perovskite $CH_3NH_3SnI_3$ degrades, which is accompanied not only by a change in morphology and the formation of voids, but also by diffusion of elements from the ITO substrate, which leads to their chemical interaction with the perovskite layer. The XPS measurements show that the decomposition process proceeds in two stages. At the first stage, at short exposure times, the photochemical and thermochemical degradation of Sn-based hybrid perovskite occurs probably with the formation of a SnI_4 as a decay product. The theoretical modeling suggests that this process is reversible. At the second stage, the oxygen, tin and indium atoms diffuse under long exposure times, which is accompanied by additional formation of Sn^{4+} ions as a result of oxidation of tin atoms. When replacing the ITO-substrate with SiO_2 such an effect is not observed and as shown by XPS study of $SiO_2/CH_3NH_3SnI_3$ annealed at 300 hours the second stage of degradation is not recorded. Theoretical modeling demonstrates that the energy required for the formation of oxygen vacancies in ITO is about two times smaller than in SiO_2 that explain the difference in thermal stability of $CH_3NH_3SnI_3$ prepared on ITO and SiO_2 substrates. Here we note that our XPS experimental data support the ionic migration from the substrate to the perovskite layer. However, the absolute value and reaction rates demonstrating migration should be taken with caution. Since in an earlier work with a glass substrate and lead perovskite, XPS measurements of irradiated and annealed $SiO_2/MAPbI_3$ also showed that contribution of substrate increases with aging time for more degraded samples.[25] Such an increase may be due to the degradation of perovskite under the influence of these external influences (light and temperature) because of the destruction of the organic cation and formation of voids as a result of which the substrate elements become visible.

AUTHOR INFORMATION

Corresponding Author

*E-mail: i.s.zhidkov@urfu.ru

Author Contributions

The manuscript was written through contributions of all authors. All authors have given approval to the final version of the manuscript.

Funding Sources

This work is supported by Russian Science Foundation (project 19-73-30020). The XPS measurements were supported by Russian Foundation for Basic Research (Project 20-42-660003) and Ministry of Education and Science of Russia (Act 211, Agreement No.02.A03.21.0006) and Theme “Electron” № AAAA-A18-118020190098-5.

Notes

The authors declare no competing financial interest

REFERENCES

[1] Duan, J.; Xu, H.; Sha, W. E. I.; Zhao, Y.; Wang, Y.; Yang, X; Tang, Q. Inorganic perovskite solar cells: an emerging member of the photovoltaic community. *J. Mater. Chem. A* **2019**, *7*, 21036-21068.

[2] Nakazaki, J.; Segawa, H. Evolution of organometal halide solar cells. *J. Photochem. Photobiol. C* **2018**, *35*, 74-107.

[3] Mehmood, H.; Tauqeer, T.; Hussain, S. Recent progress in silicon-based solid-state solar cells. *Int. J. Electronics* **2018**, *105*, 1568-1582.

[4] Liu, C.; Li, W.; Fan, J.; Mai, Y. A brief review on the lead element substitution in perovskite solar cells. *J. Energy Chem.* **2018**, *27*, 1054-1066.

[5] Wang, K.; Liang, Z.; Wang, X.; Cui, X. Lead Replacement in $CH_3NH_3PbI_3$ Perovskites. *Adv. Electr. Mater.* **2015**, *1*, 1500089.

[6] Stoumpos, C. C.; Malliakas, C. D.; Kanatzidis, M. G. Semiconducting Tin and Lead Iodide Perovskites with Organic Cations: Phase Transitions, High Mobilities, and Near-Infrared Photoluminescent Properties. *Inorg. Chem.* **2013**, *52*, 9019-9038.

[7] Takahashi, Y.; Obara, R.; Lin, Z. Z.; Takahashi, Y.; Naito, T.; Inabe, T.; Ishibashi, S.; Terakura, K. Charge-Transport in Tin-Iodide Perovskite $CH_3NH_3SnI_3$: Origin of High Conductivity. *Dalton Trans.* **2011**, *40*, 5563.

[8] Takahashi, Y.; Hasegawa, H.; Takahashi, Y.; Inabe, T. Hall mobility in tin iodide perovskite $CH_3NH_3SnI_3$: Evidence for a doped semiconductor. *J. Solid State Chem.* **2013**, *205*, 39.

[9] Gupta, S.; Cahen, D.; Hodes, G. How SnF_2 Impacts the Material Properties of Lead-Free Tin Perovskites. *J. Phys. Chem. C* **2018**, *122*, 13926-13936.

[10] Wang, F.; Ma, J.; Xie, F.; Li, L.; Chen, J.; Fan, J.; Zhao, N. Organic Cation-Dependent Degradation Mechanism of Organotin Halide Perovskites. *Adv. Funct. Mater.* **2016**, *26*, 3417–3423.

[11] Climent-Pascual, E.; Hames, B. C.; Moreno-Ramırez, J. S.; Alvarez, A. L.; Juarez-Perez, E. J.; Mas-Marza, E.; Mora-Sero, I.; de Andres, A.; Coya, C. Influence of the substrate on the bulk properties of hybrid lead halide perovskite films. *J. Mater. Chem. A* **2016**, *4*, 18153-18163.

[12] Ahmad, Z.; Najeeb, M. A.; Shakoor, R. A.; Alashraf, A.; Al Muhtaseb, S. A.; Soliman, A.; Nazeerudd M. K., Instability in $CH_3NH_3PbI_3$ perovskite solar cells (PSC) due to elemental migration and chemical composition changes. *Sci. Rep.* **2017**, *7*, 15406-15413.

[13] Soler, J. M.; Artacho, E.; Gale, J. D.; Garsia, A.; Junquera, J.; Orejon, P.; Sánchez-Portal, D. The SIESTA Method for ab initio order-N Materials Simulation. *J. Phys.: Condens. Matter* **2002**, *14*, 2745-2779.

[14] Perdew, J. P.; Burke, K.; Ernzenhorf, M. Generalized gradient approximation made simple. *Phys. Rev. Lett.* **1997**, *78*, 1396-1400.

[15] Troullier, O. N.; Martins, J. L. Efficient Pseudopotentials for Plane-Wave Calculations. *Phys. Rev. B* **1991**, *43*, 1993-2006.

[16] Junquera, J.; Paz, Ó.; Sánchez-Portal, D. Numerical Atomic Orbitals for Linear-Scaling Calculations. *Phys. Rev. B* **2011**, *64*, 235111.

[17] Boukhvalov, D. W.; Zhidkov, I. S.; Akbulatov, A. F.; Kukharenko, A. I.; Cholakh, S. O.; Stevenson, K. J.; Troshin, P. A.; Kurmaev, E. Z. Thermal Effects and Halide Mixing of Hybrid Perovskites:MD and XPS studies. *J. Phys. Chem. A* **2020**, *124*, 135-140.

[18] https://materials.springer.com/isp/crystallographic/docs/sd_0553077

[19] Zatsepin, A. F.; Zatsepin, D. A.; Boukhvalov, D. W.; Kuznetsova, Yu. A.; Gavrilov, N. V.; Shur, V. Ya.; Esin, A. A. Combined XPS, PL and DFT study of Gd-passivation of oxygen in KUVI-SiO_2 host-matrix. *J. Alloys Compd.* **2019**, *796*, 77-85.

[20] Juarez-Perez, E. J.; Hawash, Z.; Raga, S. R.; Ono, L. K.; Qi, Y. Thermal degradation of $CH_3NH_3PbI_3$ perovskite into NH_3 and CH_3I gases observed by coupled thermogravimetry - mass spectrometry analysis. *Energy Environ. Sci.* **2016**, *9*, 3406-3410.

[21] Juarez-Perez, E. J.; Ono, L. K.; Maeda, M.; Jiang, Y.; Hawash, Z.; Qi, Y. Photodecomposition and thermal decomposition in methylammonium halide lead perovskites and inferred design principles to increase photovoltaic device stability. *J. Mater. Chem. A* **2018**, *6*, 9604-9612.

[22] Kerner, R. A.; Rand, B. P. Electrochemical and Thermal Etching of Indium Tin Oxide by SolidState Hybrid Organic–Inorganic Perovskites. *ACS Appl. Energy Mater.* **2019**, 2, 6097-6101.

[23] Luchkin, S. Yu.; Akbulatov, A. F.; Frolova, L. A.; Griffin, M. P.; Dolocan, A.; Gearba, R.; Vanden Bout, D. A.; Troshin, P. A.; Stevenson, K. J. Reversible and Irreversible Electric Field Induced Morphological and Interfacial Transformations of Hybrid Lead Iodide Perovskites. *ACS Appl. Mater. Interfaces* **2017**, 9, 33478-33483.

[24] Juarez-Perez, E. J.; Ono, L. K.; Uriarte, I.; Cocinero, E. J.; Qi, Y. Degradation Mechanism and Relative Stability of Methylammonium Halide Based Perovskites Analyzed on the Basis of Acid-Base Theory. *ACS Appl. Mater. Interfaces* **2019**, *11*, 12586-12593.

[25] Zhidkov, I. S.; Poteryaev, A. I.; Kukharenko, A. I.; Finkelstein, L.D.; Cholakh, S. O.; Akbulatov, A. F.; Troshin, P. A.; Chueh, C.-C.; Kurmaev, E. Z. XPS evidence of degradation mechanism in $CH_3NH_3PbI_3$ hybrid perovskite. *J. Phys.: Condens. Matter* **2020**, 32, 095501.

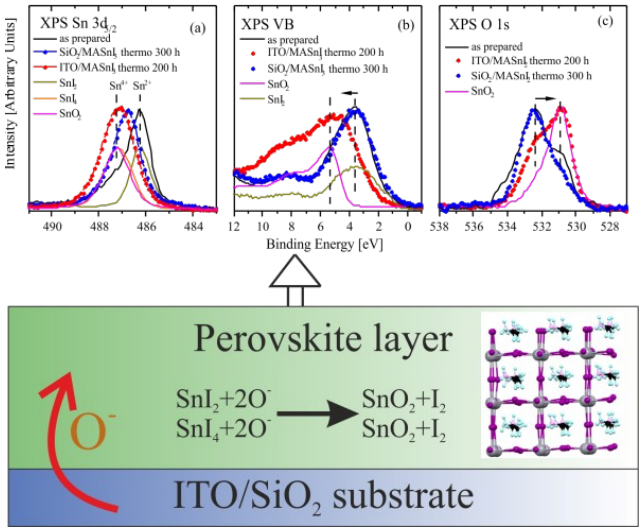
XPS Sn 3d5/2
(a)
as prepared
SiO2/MASnI3 thermo 300 h
ITO/MASnI3 thermo 200 h
SnI2
SnI4
SnO2
Sn4+ Sn2+
XPS VB
(b)
as prepared
ITO/MASnI3 thermo 200 h
SiO2/MASnI3 thermo 300 h
SnO2
SnI2
XPS O 1s
(c)
as prepared
ITO/MASnI3 thermo 200 h
SiO2/MASnI3 thermo 300 h
SnO2
Intensity [Arbitrary Units]
490 488 486 484
12 10 8 6 4 2 0
538 536 534 532 530 528
Binding Energy [eV]
Perovskite layer
SnI2+2O-
SnI4+2O-
SnO2+I2
SnO2+I2
O-
ITO/SiO2 substrate